Physics Letters B 840 (2023) 137871

Contents lists available at ScienceDirect

Physics Letters B

journal homepage: www.elsevier.com/locate/physletb

Low-p_T quarkonium polarization measurements: Challenges and opportunities

Pietro Faccioli [a,*], Ilse Krätschmer [b], Carlos Lourenço [c]

[a] LIP, Lisbon, Portugal
[b] ISTA, Klosterneuburg, Austria
[c] CERN, Geneva, Switzerland

ARTICLE INFO

Article history:
Received 20 January 2023
Received in revised form 19 February 2023
Accepted 20 March 2023
Available online 23 March 2023
Editor: M. Pierini

Keywords:
Quarkonium polarization
AMBER
Pion parton distribution functions

ABSTRACT

Several fixed-target experiments reported J/ψ and Υ polarizations, as functions of Feynman x (x_F) and transverse momentum (p_T), in three different frames, using different combinations of beam particles, target nuclei, and collision energies. Despite the diverse and heterogeneous picture formed by these measurements, a detailed look allows us to discern qualitative physical patterns that inspire a simple empirical model. This data-driven scenario offers a good quantitative description of the J/ψ and $\Upsilon(1S)$ polarizations measured in proton- and pion-nucleus collisions, in the $x_F \lesssim 0.5$ domain: more than 80 data points (not statistically independent) are well reproduced with only one free parameter. This study sets the context for future low-p_T quarkonium polarization measurements in proton- and pion-nucleus collisions, such as those to be made by the AMBER experiment, and shows that such measurements provide significant constraints on the poorly-known parton distribution functions of the pion.

1. Introduction

Studies of the production of heavy quarkonia (charm or beauty quark-antiquark states) provide an ideal path for a detailed understanding of the strong interaction in quantum chromodynamics (QCD) [1], thanks to the generally-agreed reasoning that the charm and beauty quarks are heavy enough to allow the factorization of short- and long-distance effects. Within the non-relativistic QCD (NRQCD) framework [2], in particular, the production of the $Q\overline{Q}$ pre-resonance is characterized by cross sections (short-distance coefficients, SDCs) that can be obtained through perturbative QCD computations, while the hadronization step is described by phenomenological parameters (long-distance matrix elements, LDMEs), determined from fits to experimental data. While in NRQCD the $Q\overline{Q}$ pre-resonance can have all possible configurations of spin, angular momentum, and colour, in the colour-singlet model (CSM) [3,4] it must have the same quantum numbers as the final state. The colour-evaporation model (CEM) [5,6], on the other hand, assumes that the probability of forming a specific quarkonium state is independent of the kinematics and spin of the state, as well as of the production process.

The *polarization* of the quarkonium state provides particularly significant information regarding the hadronization model, given that it directly reflects the mixture (and polarizations) of the contributing pre-resonance configurations. The polarizations of five vector quarkonia (J/ψ, $\psi(2S)$, $\Upsilon(1S)$, $\Upsilon(2S)$ and $\Upsilon(3S)$) have recently been measured at relatively high transverse momentum, p_T, at the Tevatron [7] and the LHC [8–12]. These measurements have been addressed in many studies, including analyses based on the NRQCD [13–20] and CEM [21] approaches.

In this paper we devote our attention to low-p_T quarkonium hadro-production, a kinematical domain complementary to that explored in collider experiments. The J/ψ production cross sections measured (as a function of longitudinal momentum) in proton- and pion-induced fixed-target collisions have been analysed in considerable detail in two recent studies, made in the framework of the CEM [22] and of the NRQCD framework [23]. One of the main results of these studies is that charmonium cross section measurements in pion-induced collisions are a sensitive probe of the gluon distribution function in pions. The study reported in this article is complementary with respect to those studies in two crucial aspects. First, we consider the measured quarkonium polarizations rather than the cross sections. Second, in our evaluation of potential inconsistencies among data sets and in our extrapolations to the conditions of future measurements, we adopt a simple

* Corresponding author.
E-mail addresses: pietro.faccioli@cern.ch (P. Faccioli), carlos.lourenco@cern.ch (C. Lourenço).

https://doi.org/10.1016/j.physletb.2023.137871

empirical model based on hypotheses directly inspired by the experimental data.

We start by listing and reviewing the J/ψ and Υ(nS) polarization measurements reported by fixed-target experiments at CERN, DESY, and Fermilab, using proton or pion beams in a broad energy range, and targets made of several materials. We then evaluate if these results can be considered to be consistent with each other, without evidence of mutually-contradicting data, so that they can be used to set the context for future measurements (such as those to be made by the AMBER experiment [24]). Such an analysis is not straightforward, in particular because most of the results were obtained through one-dimensional analyses (ignoring the azimuthal decay angle) and were reported using three different polarization frames, besides being obtained in a rather diverse set of collision energies, kinematical ranges, beam and target species, etc. We solve this problem by considering a simple model of low-p_T quarkonium production, directly inspired by the patterns emerging from a careful look at the experimental results, which clearly indicate some tendencies towards significant polarizations in certain kinematical regions. We then use this empirical model to describe the existing data, fixing a single free parameter, and make predictions for future polarization measurements, showing, in particular, that they can provide significant constraints in future determinations of the parton distribution functions (PDFs) of the pion. We emphasise that this study is exclusively focused on the polarization measurements and deliberately follows an empirical approach. Analyses of low-p_T cross sections based on the NRQCD and CEM approaches can be found in Refs. [22,23,25–29].

The paper is structured as follows. Section 2 presents the experimental measurements we have considered. Section 3 discusses the qualitative indications of the data patterns, which are then developed in Section 4 into a simple empirical model. Quantitative comparisons between the model and the experimental measurements are shown in Sections 5 and 6, while predictions for future experiments are provided in Section 7.

2. Experimental data

Figs. 1 and 2 present, respectively for the J/ψ and Υ states, polarization measurements made by fixed-target experiments, listed in Table 1, using proton or pion beams and several target materials. The considered observable, shown as functions of x_F and p_T, is the polar anisotropy parameter λ_ϑ [30]. Most of the measurements concern the J/ψ meson [31–42], only one regarding Υ production [43]. The ensemble of experiments covers an overall kinematical domain defined by $-0.3 \lesssim x_F \lesssim 1$ and $0 < p_T \lesssim 5$ GeV, with average p_T between 1.0 and 1.2 GeV and average p_T squared in the $1.5 \lesssim \langle p_T^2 \rangle \lesssim 2.2\,\text{GeV}^2$ range.

The polarizations were measured in three different frames: Collins–Soper (CS) [44], Gottfried–Jackson (GJ) [45] and centre-of-mass helicity (HX), where the polarization axis z is defined, respectively, as the relative direction of the colliding nucleons, the direction of one of the two nucleons (generally the beam proton), and the direction of the quarkonium itself with respect to the centre-of-mass of the system of the two nucleons [30].

Each experiment measured the polarization of J/ψ mesons using different combinations of beam particles, target nuclei, and collision energy. The collision energies span the range from $\sqrt{s} = 15.3$ to 41.6 GeV, while the target nuclei include eight elements, between hydrogen and tungsten. The beam particles include pions (both charges), protons and antiprotons, and even indium nuclei. And in the case of secondary beams (e.g., the pion and antiproton cases), the beam composition is contaminated by some fraction of other particles, which adds further complexity to the picture. These complications can be illustrated with a few examples. E444 collected data with a beam composed of several particles ($\pi^\pm$, $K^\pm$, p, $\bar{p}$) hitting a target system composed of several materials (C, Cu, W), the combination π^--C being the most important. WA11 collected 40% of the data at 140 GeV beam momentum and 60% at 150 GeV. E537 collected data with several beam-target configurations; the J/ψ sample is dominated by the π^--W combination but there is also an important contribution (around 25% of the events) from $\bar{p}$-W collisions, while the data collected with Be and Cu targets, with both beams, is a negligible contamination.

Besides the diversity of collision energies, beam particles, and target nuclei, which surely contributes to the visible spread of the data points, we also need to take into consideration that polarization measurements are always very challenging and it is quite possible that some of the reported systematic uncertainties are underestimated (in fact, some of the older results were even published without mentioning systematic uncertainties). In particular, most of the measurements were obtained from one-dimensional

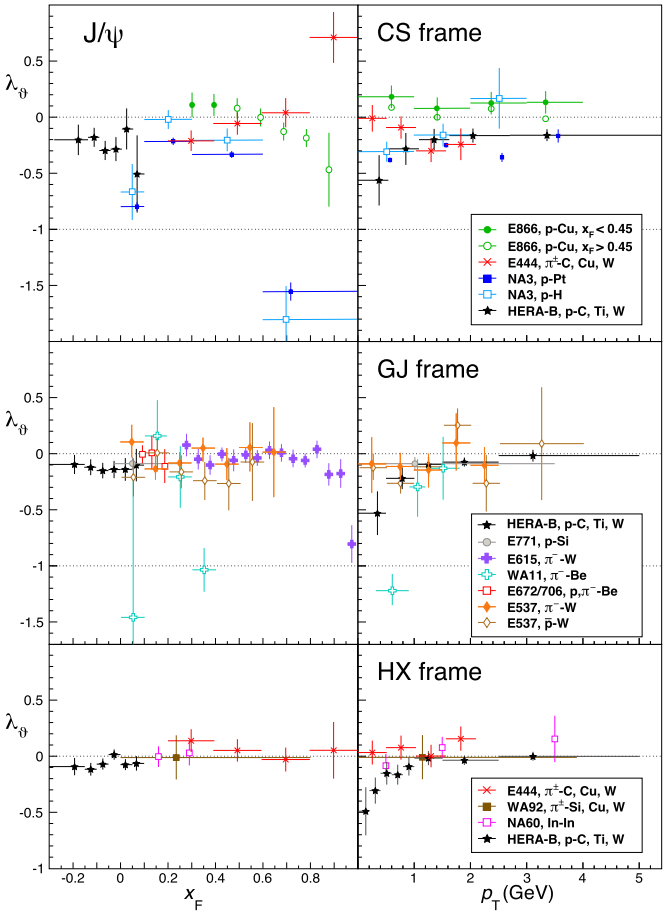

Fig. 1. The J/ψ polar anisotropy parameter λ_ϑ measured in the CS, GJ, and HX frames (top to bottom), vs. x_F and p_T.

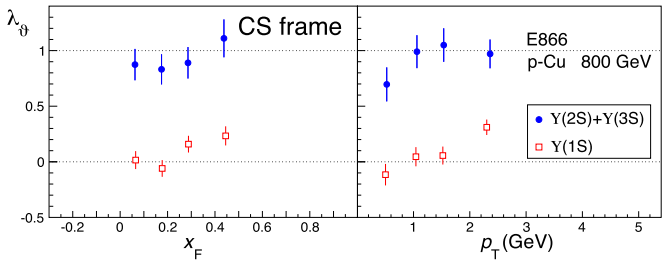

Fig. 2. The Υ(1S) and Υ(2S+3S) polar anisotropy parameter λ_ϑ measured by E866 in the CS frame, vs. x_F and p_T.

Table 1
J/ψ and Υ polarization measurements in fixed target experiments, characterized by several beam energies ($E_{\rm lab}$) and angular coverages, denoted using $x_{\rm F}$, centre-of-mass rapidity ($y_{\rm cms}$) or fractional momentum of the beam partons (x_1).

Exp. [Ref.]	Beam	Target	$E_{\rm lab}$ (GeV)	$\sqrt{s}$ (GeV)	$\Delta x_{\rm F}$	$\Delta p_{\rm T}$ (GeV)	$\langle p_{\rm T}\rangle$, $\langle p_{\rm T}^2\rangle$ (GeV), (GeV^2)
				J/ψ			
E537 [31]	π^-, $\bar{\rm p}$	W	125	15.3	0.0–0.7	0–2.5	$\langle p_{\rm T}\rangle = 1.04$
WA11 [32]	π^-	Be	146	16.6	0.0–0.4	0–2.4	$\langle p_{\rm T}\rangle = 1.0$
NA60 [33]	In	In	158	17.2	$y_{\rm cms}$: 0–1	$\approx$0–4	
E444 [34]	$\pi^\pm$	C, Cu, W	225	20.6	x_1: 0.2–1.0	0–2.5	$\langle p_{\rm T}\rangle = 1.2$
E615 [35]	$\pi^\pm$	W	252	21.8	0.25–1.0	0–5	
NA3 [36]	π^-	H, Pt	280	22.9	0.0–1.0		$\langle p_{\rm T}^2\rangle = 1.52, 1.85$
WA92 [37]	π^-	Si, Cu, W	350	25.6	$\approx$0.0–0.8	0–4	
E672/706 [38]	π^-	Be	515	31.1	0.1–0.8	0–3.5	$\langle p_{\rm T}\rangle = 1.17$
E672/706 [39]	p	Be	530, 800	31.5, 38.8	0.0–0.6		$\langle p_{\rm T}\rangle = 1.15, 1.22$
E771 [40]	p	Si	800	38.8	−0.05–0.25	0–3.5	$\langle p_{\rm T}^2\rangle = 1.96$
E866 [41]	p	Cu	800	38.8	$\approx$0.0–0.5	$\approx$0–4	
HERA-B [42]	p	C, Ti, W	920	41.6	−0.34–0.14	0–5.4	$\langle p_{\rm T}^2\rangle = 2.2$
				Υ(1S) and Υ(2S)+Υ(3S)			
E866 [43]	p	Cu	800	38.8	0.0–0.6	0–4	$\langle p_{\rm T}\rangle = 1.3$

analyses, only considering the $\cos\vartheta$ observable and neglecting acceptance correlations between the $\cos\vartheta$ and φ variables of the dilepton angular distribution, a practice that can easily lead to significantly biased results, as discussed in Refs. [30,46]. This might explain why some of the data points shown in Fig. 1 are outside of the physically allowed range (with $\lambda_\vartheta < -1$).

Despite the first impression that the data points form a rather scattered overall picture, we can see that most of the J/ψ values fluctuate around the $\lambda_\vartheta = 0$ limit (unpolarized production), with some trends towards strong polarizations in certain regions of the kinematic domain. Among the J/ψ measurements, the one published by HERA-B [42] stands out as the only one that considers all three polarization frames (CS, GJ and HX) and that, furthermore, includes all three shape parameters of the angular distribution relevant for parity-conserving decays: λ_ϑ, λ_φ and $\lambda_{\vartheta\varphi}$ [30]. It will, therefore, provide a very useful beacon to guide our extraction of physically relevant trends (presented in the next section) from the diverse data collection.

The most salient feature that one can easily see as standing out of the global picture is the polarization measurement reported by E866 for the (unresolved) Υ(2S) plus Υ(3S) states [43]. While the values reported for the Υ(1S) mesons produced with $x_{\rm F} < 0.45$ cluster around $\lambda_\vartheta \sim 0.1$ and are consistent with the J/ψ values provided by the same experiment, for identical experimental conditions [41], those reported for the 2S+3S states are surprisingly different: $\lambda_\vartheta \sim +1$. If we exclude the possibility of problems with the experimental measurement, this observation reveals an astounding difference between the polarizations observed for the excited states and for the ground state. Given that these three S-wave states are expected to have identical polarizations when directly produced (or when produced in decays of heavier S-wave states [47–49]), the observed difference, $\lambda_\vartheta(2S+3S) - \lambda_\vartheta(1S) \sim 1$, seems to be almost impossible to reproduce, even resorting to extreme hypotheses for the polarizations of the χ_{bJ}(nP) states and their (possibly very different) feed-down contributions to the production of the three vector states (at least in the kinematical conditions of these low $p_{\rm T}$ measurements).

This observation justifies that, in the study reported in this paper, we developed our empirical model (and determined its only free parameter) exclusively on the basis of the J/ψ data. It is only a posteriori that we compare the outcome of the computations to the Υ patterns and discuss what one can infer from that comparison. Our reluctance in using the remarkable $\lambda_\vartheta(2S+3S) - \lambda_\vartheta(1S) \sim 1$ difference as an *input* of our study is exclusively based on a principle of caution. Polarization measurements are always challenging and this case is even more demanding because the dimuon mass distribution reported by E866 is affected by a poor measurement resolution and a daunting signal-to-background ratio, so that the (unresolved) 2S and 3S states are not visible as a peak on the top of the underlying continuum. In contrast, the Υ(1S), Υ(2S) and Υ(3S) polarizations measured by CMS [9], in much more favourable experimental conditions, do not show any differences between the three S-wave states. Clearly, if the patterns shown in Fig. 2 are not disturbed by experimental difficulties, their comparison to the CMS results points to the importance of the different experimental conditions: the collision energy, the longitudinal and transverse momentum ranges, and the use of a nuclear target (Cu) in the E866 data. In any case, it would certainly be very useful to have the fixed-target measurement repeated by another experiment, with improved detection capabilities.

3. Qualitative physical indications

The empirical model presented in this paper, described in the next section and then quantitatively tested in Section 5, is inspired by two qualitative physical observations revealed by the J/ψ polarization patterns.

The first observation follows from the HERA-B measurements [42], which provide the three shape parameters (λ_ϑ, λ_φ, and $\lambda_{\vartheta\varphi}$) in three polarization frames (CS, GJ, and HX). As suggested by the global picture of J/ψ measurements presented in Fig. 1 and more clearly and precisely seen in the top panels of Fig. 3, the magnitude of the polar anisotropy parameter λ_ϑ is systematically larger in the CS frame and smaller in the HX frame. At the same time, as shown in the bottom panels of Fig. 3, the azimuthal anisotropy parameter λ_φ increases in magnitude following the inverse hierarchy, being the largest in the HX frame and the smallest in the CS frame. It is important to appreciate that the differences between the values measured in the three frames *are* significant, contrary to what the displayed uncertainties could indicate at first sight, because the three sets of data points were obtained using exactly the same events and, hence, their statistical uncertainties are fully correlated. The only uncertainties affecting the *differences* between the three sets of parameters are the frame-dependent systematic uncertainties, presumably much smaller than those represented by the error bars, so that the differences are certainly larger than zero.

These λ_ϑ and λ_φ frame hierarchies reflect the geometrical difference between the three frame definitions. To start with, the GJ polarization axis has always, for every $p_{\rm T}$ and $x_{\rm F}$, a direction between the CS and HX axes. More importantly, the sequence of the hierarchy, with the CS frame showing the largest polarization and the smallest azimuthal anisotropy, has one clear physical inter-

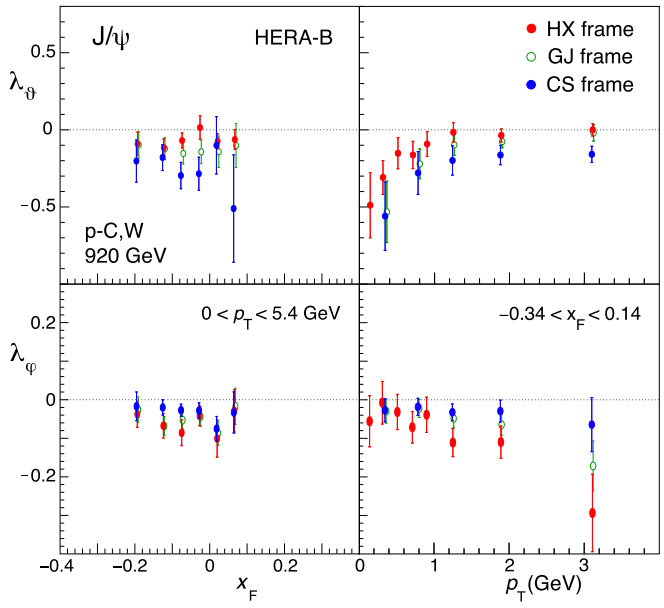

Fig. 3. The J/ψ λ_ϑ and λ_φ parameters measured by HERA-B in the CS, GJ and HX frames, vs. x_F and p_T.

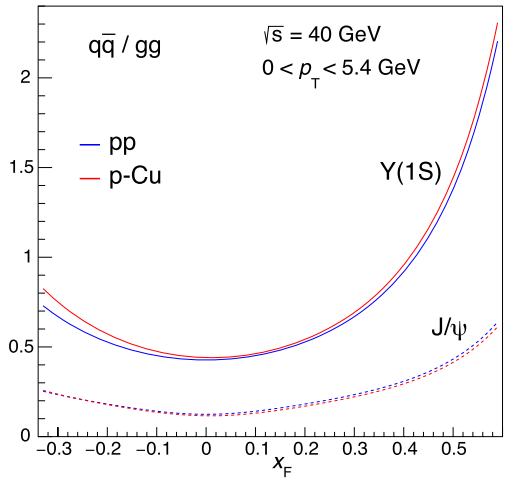

Fig. 4. The $q\bar{q}$ to gg parton luminosity ratios for J/ψ and Υ(1S) production, vs. x_F, illustrated for conditions similar to those of the E866 and HERA-B experiments.

pretation: the CS axis is the one that most naturally reflects the alignment of the J/ψ angular momentum [50]. This observation provides important information regarding the topological nature of the involved processes: they must be, predominantly, of the 2-to-1 kind ($h_1\,h_2 \to$ J/ψ), where the produced object directly inherits the angular momentum state of the system of colliding partons, which is polarized along the direction of the collision. Indeed, in 2-to-2 processes the polarization legacy of the partons is shared between the two final objects and, while the angular momentum balance is more complex and depends on the coupling of the final states to the intermediate virtual particles, one can generally say that a natural alignment along the direction of the colliding partons is excluded. As a result, the CS frame starts showing a reduced polar anisotropy and a non-zero azimuthal component. So, the observed polarization hierarchy reinforces the idea that 2-to-2 channels have a negligible contribution to low-p_T quarkonium production, possibly indicating that most of the mesons produced in such processes ($h_1\,h_2 \to$ J/$\psi + X$, where the J/ψ is emitted with a recoil hadron) have a minor role for p_T values smaller or comparable to the intrinsic momenta of the colliding partons.

An interesting illustration is provided by Drell–Yan (DY) production [51]. At the lowest order, DY production is a 2-to-1 process, characterized by a "natural" polarization along the collision direction, approximated by the CS axis. Instead, 2-to-2 processes (t- or s-channel) naturally lead to polarizations along the GJ and HX axes. In the case of quarkonium production, the final state (the experimentally observable quarkonium state) evolves from an intermediate (singlet or octet) $Q\,\overline{Q}$ pre-resonance state, through the possible emission of one or more soft gluons. But the emission of one soft gluon (or more) in the bound state formation process does not qualify the process as "2-to-2", given that we are talking about the process that produces the $Q\,\overline{Q}$ state: the emitted gluon is not to be seen as a final-state object of a 2-to-2 topology. Indeed, as long as the mass difference between the real final state and the virtual intermediate state is smaller than the total momentum, $[(s/4)\,x_F^2 + p_T^2]^{1/2}$, of the observed state in the centre-of-mass of the colliding nucleons, the natural polarization direction of the final state coincides with the one of the intermediate state (that is, the direction of the colliding partons, in 2-to-1 processes), as discussed in Ref. [52] for the case of the radiative χ_c decays to J/ψ. Given these considerations, it is not difficult to accept the evidence, provided by the frame hierarchy shown by data, that low-p_T quarkonium production is dominated by 2-to-1 scattering processes, $gg \to Q\,\overline{Q}$ and $q\bar{q} \to Q\,\overline{Q}$, leading to strongly polarized quarkonia.

The second experimental indication is the observation of trends towards longitudinal J/ψ polarization at small $|x_F|$ ("mid-rapidity"). It is reasonable to suppose that this behaviour is correlated with the relative dominance of gluon-gluon fusion at mid-rapidity, the $q\bar{q}$ annihilation process becoming more relevant as we move towards the forward region. This hypothetical correlation can be appreciated by looking at the ratio between the $q\bar{q}$ and the gg "luminosities", each computed as the product of the corresponding parton distribution functions (PDFs). Fig. 4 shows the x_F dependence of such a ratio, computed for the J/ψ and Υ(1S) cases, for $\sqrt{s} = 40$ GeV, using the CT14NLO [53] set of proton PDFs, as provided by the LHAPDF library [54]. The p-Cu curves were computed with the target PDFs (both for the protons and for the neutrons) modified to reflect nuclear effects, using the EPPS16 package [55]; for the collision energies of the E866 and HERA-B experiments, the nuclear effects on the PDFs play a negligible role. We clearly see that, as expected, the ratio has a minimum in the $x_F \sim 0$ region and increases as we move away from mid-rapidity. It is also clear that the ratio is considerably higher for the Υ(1S) than for the J/ψ, reflecting the fact that, relatively speaking, $q\bar{q}$ annihilation becomes more important in the production of heavier particles. This is another hint that $q\bar{q}$ annihilation leads to transversely polarized quarkonia, given that, overall, the measurements collected in Figs. 1 and 2 (at least within the $x_F \lesssim 0.5$ range) indicate that the observed polarizations are more transverse for the Υ states than for the J/ψ.

This correlation between the measured quarkonium polarization patterns and the relative importance of the gg and $q\bar{q}$ luminosities is the central motivation of our hypothesis that gg fusion produces longitudinally polarized mesons while those produced through $q\bar{q}$ annihilation are transversely polarized. A physical justification supporting this assumption is beyond the scope of this paper, where we take a data-driven approach and let the measured patterns be our guiding principles. Nevertheless, it is not difficult to conceive that $q\bar{q}$-induced J/ψ and Υ production might be analogous to the DY case and that, therefore, those quarkonia should be transversely polarized (angular momentum projection $J_z = \pm 1$) because of helicity conservation in the coupling between the annihilating quarks and a gluon. The longitudinal polarization of the quarkonia produced in gg fusion, on the other hand, can be justified, for example, with a dominating $J_z = 0$ projection of the gg

system (then inherited by the $Q\overline{Q}$ state), which is a necessary condition, forced by angular momentum conservation, if the scattering gluons are transversely polarized and form a $J = 1$ state.

In summary, the data patterns seen in Figs. 1 and 3 indicate that: 1) 2-to-1 processes dominate; and 2) quarkonia produced in gg fusion have longitudinal polarization and those produced in $q\overline{q}$ annihilation have transverse polarization.

Before concluding this section, it is important to note that our study is exclusively devoted to quarkonium production in the $x_F \lesssim 0.5$ domain and does not address the high x_F region, where a trend towards longitudinal polarization has been seen by E615 and E866 (in pion- and proton-nucleus collisions, respectively). Although certainly interesting in their own right [56,57], this edge of phase space is likely to be dominated by processes that are not covered by the model that we discuss in this paper.

4. Description of the empirical model

As anticipated in the previous section, our empirical model is based on two assumptions. 1) $Q\overline{Q}$ production is dominated by 2-to-1 topologies, so that contributions producing at least one additional object besides the quarkonium, are considered negligible. It is worth noting that qg scattering, in particular, is expected to have a negligible contribution to the total production cross section [22] and, furthermore, quarkonia produced through this process, always with other final-state particles, are not expected to directly reflect the spin alignments of the colliding particles and tend, therefore, to have less significant polarizations than those produced in 2-to-1 processes. 2) The $gg \to Q\overline{Q}$ and $q\overline{q} \to Q\overline{Q}$ processes lead, respectively, to fully longitudinal and fully transverse polarizations of the *directly produced* J/ψ, $\psi(2S)$, and Υ mesons. For these "natural" polarizations we assume as quantization axis the (unobservable) relative direction of the colliding partons, which does not coincide (event-by-event) with the CS axis because of the (small but) nonzero parton transverse momenta, $\vec{k}_{1T}$ and $\vec{k}_{2T}$.

In fact, for measurements performed at low p_T, small $|x_F|$, and light particles (such as the J/ψ), the transverse component of the parton motion inside the colliding hadrons has an effect on the observable polarization. For the scope of the present discussion, we will assume that the parton k_T reaches a magnitude $\langle k_T^2 \rangle = \mathcal{O}(1\,\mathrm{GeV}^2)$, compatible with the measured p_T distributions: $\langle p_T^2 \rangle \simeq 2\,\langle k_T^2 \rangle \simeq 2\,\mathrm{GeV}^2$ (see, e.g., Ref. [58]). This effectively means that the meaning of $\vec{k}_T$ is extended with respect to the bare intrinsic momentum owned by partons for being confined inside a hadron of finite dimensions ($\Delta p \sim 1/(1\,\mathrm{fm}) = 0.2\,\mathrm{GeV}$), by also considering extra sources of transverse momentum kick occurring during the scattering process (soft gluon emissions, multiple scattering in the nuclear target, etc.). The parton transverse momenta also provide the only source of quarkonium p_T considered in the model.

The vectors $\vec{k}_{1T}$ and $\vec{k}_{2T}$ are generated in space, with the two moduli following a Gaussian distribution of variance $\langle k_T^2 \rangle = 1\,\mathrm{GeV}^2$ and the azimuthal angles ϕ_1 and ϕ_2 following uniform distributions. While the $\vec{k}_T$ effect has a negligible influence for Υ production, it has a significant impact in the observable J/ψ polarization, as illustrated in Fig. 5 for fully transverse (solid lines) and fully longitudinal (dashed lines) natural polarizations, for $\sqrt{s} = 40\,\mathrm{GeV}$. We see that the magnitude of the λ_ϑ parameter measured in the CS frame is reduced with respect to the values generated in the parton-parton frame, by about 20% and 10% for the fully transverse and fully longitudinal polarizations, respectively.

As expected, the CS frame remains the best approximation of the natural frame: the λ_ϑ values observable in the GJ and HX frames depart more significantly from the generated one. The λ_φ values are presented in the bottom panels of Fig. 5, showing the same inverted hierarchy that we have seen in the HERA-B results. There is a nonzero λ_φ value also in the CS frame, as a result of the rotation from the natural frame. However, the transformation from the natural parton-parton to the "laboratory" CS frame is not a simple rotation in the production plane (around the y axis), as is the case between any two of the three experimental frames. While the magnitude of the polar anisotropy decreases exactly as in such ordinary frame rotations (for the same rotation angle), the correspondingly arising azimuthal anisotropy, $\lambda_\varphi \neq 0$, no longer geometrically compensates the $|\lambda_\vartheta^{CS}|$ decrease. In fact, in this case the rotation plane (formed by the parton-parton and proton-nucleon relative momentum directions) does not coincide with the experimentally defined production plane. The angle between the two planes changes from one event to the next, so that the azimuthal anisotropy resulting from the tilt between the natural polarization axis and the experimental axis tends to be smeared out in the integration over all events. Consequently, the invariant polarization parameter $\tilde{\lambda}$ [59,60] (shown as black curves on the top panels of Fig. 5), while slightly closer to the natural value, does not return its full magnitude: the natural polarization is unrecoverably smeared in any observation frame.

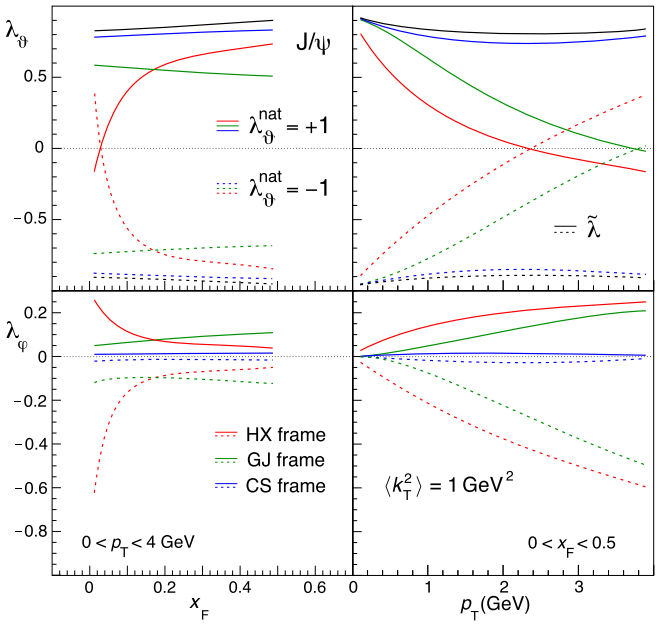

Fig. 5. The λ_ϑ and λ_φ parameters as would be observed in the CS, GJ, and HX frames for fully transverse and longitudinal J/ψ polarizations along the direction of the colliding partons, for $\sqrt{s} = 40\,\mathrm{GeV}$ and $\langle k_T^2 \rangle = 1\,\mathrm{GeV}^2$, as a function of x_F averaged over p_T (left) and vice versa (right). The invariant polarization parameter $\tilde{\lambda}$, shown in black, is by definition identical in the three observation frames.

The relative proportion of quarkonia *directly* produced through $q\overline{q}$ annihilation and gg fusion processes and, therefore, their observable mixture of longitudinal and transverse polarizations, is fully determined in the model by the product of two ratios, R and r. The first one is the ratio between the $q\overline{q}$ and gg parton densities,

$$R = \frac{\sum_q [F_1^q(x_1,\hat{s})\,F_2^{\overline{q}}(x_2,\hat{s}) + F_1^{\overline{q}}(x_1,\hat{s})\,F_2^q(x_2,\hat{s})]}{F_1^g(x_1,\hat{s})\,F_2^g(x_2,\hat{s})}\,, \tag{1}$$

where $\hat{s} = M_Q^2 + p_T^2$ and $x_1\,x_2 = \hat{s}/s$, with M_Q being the quarkonium mass and $p_T = |\vec{k}_{1T} + \vec{k}_{2T}|$; the indexes 1 and 2 refer, respectively, to the beam proton and the target nucleon, and the sum is made over the participating quark flavours ($q = u, d$). Nuclear modification factors for the nucleon in the target, different for sea and

valence quarks, are computed with the EPPS16 package [55] and applied in the definition of F_2.

The second ratio is the one between the $q\overline{q}$ and gg partonic cross sections,

$$r = \frac{\hat{\sigma}(q\overline{q} \to \mathcal{Q})}{\hat{\sigma}(gg \to \mathcal{Q})}, \tag{2}$$

assumed to be universal, that is, identical for all considered vector quarkonia, $\mathcal{Q} = J/\psi$, $\psi(2S)$, $\Upsilon(nS)$. In principle, one might be able to evaluate r within the context of specific model-dependent approaches, such as, for example, the NRQCD framework. It should be noted, however, that r is the ratio of the partonic cross sections, depending not only on the "short-distance parton-level cross sections" (the SDCs), which can be computed in perturbative QCD, but also on the probabilities of the transitions from the $Q\,\overline{Q}$ "pre-resonances" (singlet and octet states) into the final quarkonium state (the LDMEs). These probabilities represent non-perturbative evolution processes and are presently not calculated, but rather determined from global analyses of collider data. Besides, they are a priori different in the $q\overline{q}$ and gg cases, which, in general, produce pre-resonances of different angular momentum properties. In our study we deliberately try to remain as agnostic as possible regarding model-dependent inputs, so that we treat r as an empirical parameter, adjusted through the analysis of the J/ψ data.

The resulting natural polarization parameter λ (in the parton-parton CS frame), for a given mixture of $q\overline{q}$ and gg events (expressed by $R \times r$), is determined according to the sum rule presented in Eq. 11 of Ref. [30], reported here as a function of the $q\overline{q}$ and gg fractions, $f_{q\overline{q}} = R \times r/(1 + R \times r)$ and $f_{gg} = 1/(1 + R \times r)$, and of the corresponding assumed polarizations, $\lambda^{q\overline{q}}$ and λ^{gg}:

$$\lambda = \frac{f_{q\overline{q}}\,\lambda^{q\overline{q}}/(3+\lambda_\vartheta^{q\overline{q}}) + f_{gg}\,\lambda^{gg}/(3+\lambda_\vartheta^{gg})}{f_{q\overline{q}}/(3+\lambda_\vartheta^{q\overline{q}}) + f_{gg}/(3+\lambda_\vartheta^{gg})}. \tag{3}$$

This expression is explicitly x_F dependent because of the presence of R (that is, of the PDFs) in the $q\overline{q}$ and gg fractions, while a further kinematic dependence, also on p_T, is acquired by the polarization parameters when translated to the observable frames (CS and HX); this translation is performed by generating pseudo-events with a Monte Carlo method.

To turn the polarizations determined in this way, for the directly-produced quarkonium states, into values that can be compared with the measured data, we need to take into account the effect of the feed-down contributions from decays of heavier quarkonia.

Let us consider first the feed-down from excited *vector* quarkonia. As long as the mother and daughter states have the same mechanism of production from partonic scattering, the feed-down decays from heavier vector states are "invisible" from the polarization point of view. This is confirmed by the observation that the J/ψ mesons produced in $\psi(2S) \to J/\psi\,\pi\pi$ decays have the same polarization as the $\psi(2S)$ mesons themselves [47] and by the analogous observation made in the Υ family [48,49]. On the contrary, P-wave states have, in general, different production mechanisms with respect to the vector states. Moreover, the χ_c and χ_b mesons decay to the J/ψ and Υ mesons with the emission of a transversely polarized photon, which alters the spin-alignment of the $Q\,\overline{Q}$ [52]. Therefore, we should expect that the J/ψ and Υ mesons produced in decays of P-wave states have different polarizations with respect to the directly produced ones. In particular, if large fractions of the observed vector quarkonia are produced through χ feed-down decays, we should observe weaker transverse or longitudinal polarizations than what would be measured if all mesons were directly produced.

The J/ψ and Υ feed-down fractions from χ mesons depend on the experimental conditions; for example, they can be different if gg fusion or $q\overline{q}$ annihilation dominates, since different selection rules between the initial state and the final S- and P-wave states are expected in the two cases. Therefore, besides using the most reasonable ("central") feed-down scenario, we will also consider two options characterized by extreme hypotheses that, together, should represent a conservative "uncertainty band". The J/ψ and Υ feed-down scenarios have two ingredients: the feed-down fractions from decays of the χ_1 and χ_2 states, and the natural λ_ϑ values for the J/ψ or Υ mesons produced in each of those decays.

Regarding the feed-down fractions, and starting with the J/ψ case, our central scenario assumes that 19% of the observed J/ψ mesons come from χ_c decays (for both gg and $q\overline{q}$ production), corresponding to the central value of the HERA-B measurement [61]. For the two extreme scenarios, where the χ_c feed-down has a maximal impact on the observable prompt J/ψ polarization, we use the value 25%, representing an upper limit evaluated taking into account the CDF [62] and LHCb [63] measurements. The feed-down fractions in the bottomonium family are not well known, especially in the low-p_T range relevant for the fixed-target results that we are addressing in this paper. On the basis of LHCb measurements at forward rapidity [64] and of extrapolated trends of mid-rapidity LHC cross sections [65], we will assume that, for the central scenario, the $\Upsilon(1S)$ and $\Upsilon(2S{+}3S)$ results of E866 are affected by χ_b feed-down contributions of 45% and 25%, respectively; these values are increased to 60% and 50% in the extreme scenarios.

The values just mentioned are the total χ feed-down fractions, $R_{\chi_1} + R_{\chi_2}$. We obtain the two individual fractions, R_{χ_1} and R_{χ_2}, by assuming that they are identical, in the three scenarios, after verifying that variations in the range $0.6 < R_{\chi_1}/R_{\chi_2} < 1.4$, established by HERA-B [61], do not lead to significant changes in the results. We also believe that the range of hypotheses assumed for the χ feed-down fractions is wide enough to cover possible dependences of the inputs on the experimental conditions, such as the x_F and p_T ranges of the different measurements.

Concerning the polarizations, the central scenario assumes: a) that $q\overline{q}$ production leads to a (vector or P-wave) quarkonium state with angular momentum projection ± 1, i.e., $\lambda_\vartheta = -1/3$ for J/ψ or Υ mesons from χ_1 or χ_2 decays [52] (besides the already mentioned $\lambda_\vartheta = +1$ for the directly produced vector quarkonia); and b) that gg production gives angular momentum projection equal to 0, meaning $\lambda_\vartheta = -1$, $+1$, and $-3/5$, respectively for directly produced J/ψ or Υ mesons, and for those coming from χ_1 and χ_2 decays [52]. The two alternative ("extreme") scenarios are defined by the edges of the physical intervals for the polarizations of J/ψ or Υ mesons from χ_1 and χ_2 decays: $[-1/3, +1]$ and $[-3/5, +1]$, respectively. The scenarios using the most longitudinal and transverse χ polarizations are labelled as "lower" and "upper", respectively. For clarity, the natural polarizations assumed in the three scenarios are collected in Table 2. The only available measurement of χ_{c1} and χ_{c2} polarizations, recently reported by the CMS experiment [66], indicates that, at high p_T and mid-rapidity, they tend to have opposite polarizations, as in our central scenario for gg fusion.

As already mentioned, the small mass difference between the mother and daughter particles, in all considered cases, ensures that the natural angular momentum alignment direction is preserved in the decay [52]: also for indirect production we use, therefore, the parton-parton direction as quantization axis.

5. Data vs. model for p-nucleus collisions

Fig. 6 compares the HERA-B and E866 measurements of the J/ψ polarization parameters, as functions of x_F and p_T, with the corresponding curves computed with the model described in the

Table 2
Values of λ_ϑ considered in the generation of the J/ψ or Υ mesons resulting from feed-down decays of χ_1 or χ_2 mesons produced through gg fusion or $q\overline{q}$ annihilation, in the baseline "central" scenario and in two extreme scenarios, "lower" and "upper", leading, respectively, to the most longitudinal and most transverse values for the natural polarization of the total prompt-J/ψ polarization. In all scenarios, the directly-produced vector states are generated with $\lambda_\vartheta = -1$ and $+1$ for gg fusion and $q\overline{q}$ annihilation, respectively.

		$\lambda_\vartheta^{\chi_1}$	$\lambda_\vartheta^{\chi_2}$
central	gg	$+1$	$-3/5$
	$q\overline{q}$	$-1/3$	$-1/3$
lower	gg, $q\overline{q}$	$-1/3$	$-3/5$
upper	gg, $q\overline{q}$	$+1$	$+1$

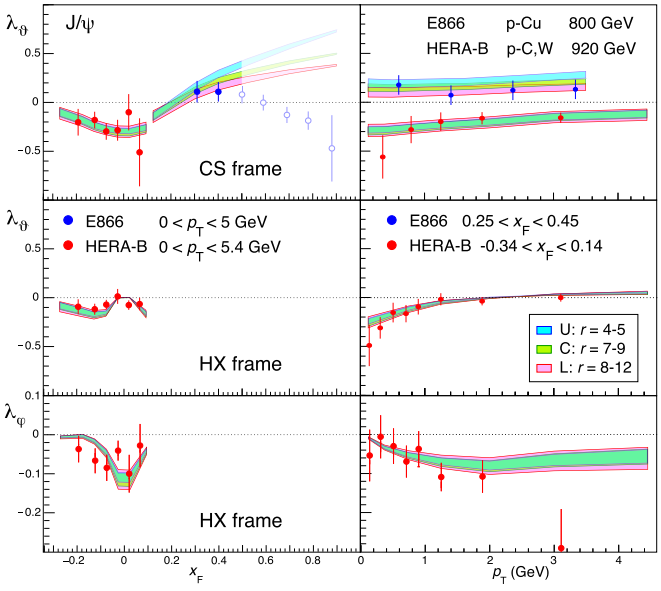

Fig. 6. The x_F (left) and p_T (right) dependences of the J/ψ polarization parameters λ_ϑ in the CS (top) and HX (middle) frames, and λ_φ in the HX frame (bottom), as measured by HERA-B (red points) and E866 (blue points). The cyan, green, and magenta bands represent, respectively, the upper (U), central (C), and lower (L) scenarios described in the text; they are independently computed for the HERA-B and E866 conditions. The departure of the bands from the E866 measurements for $x_F > 0.45$ (open circles) justifies the conjecture that our model is not valid to describe high-x_F quarkonium production.

previous section, using the central set of the CT14NLO [53] proton PDFs, properly adapting the calculations to the specific conditions (quarkonium state, collision energy, p_T and x_F coverage). The considered parameters are the λ_ϑ in the CS frame (where the model does not foresee visible deviations of λ_φ from zero, a prediction confirmed by the data, as seen in Fig. 3) and both λ_ϑ and λ_φ in the HX frame (where the two parameters share the magnitude of the natural polarization effect). For each of the three scenarios, a range of values for the only parameter not fixed by our hypotheses, the $q\overline{q}$ over gg cross section ratio, r, has been determined so as to maximize the agreement with the data within the $x_F \lesssim 0.5$ domain: the obtained ranges are 4–5, 7–9 and 8–12, for the upper, central and lower scenarios, respectively.

It is not possible to compare these data-driven evaluations of r with theory-specific values because they reflect not only the short-distance part of the processes, which are calculable (see, e.g., Refs. [67,68]), but also, and most significantly, the long-distance non-perturbative hadronization factors (LDMEs), which are unknown and presumably different for the gg and $q\overline{q}$ processes (because of angular momentum and helicity conservation, among other factors). In particular, sets of LDMEs determined using LHC measurements, for example, cannot be assumed to be applicable to the low-p_T domain of the fixed-target measurements [23].

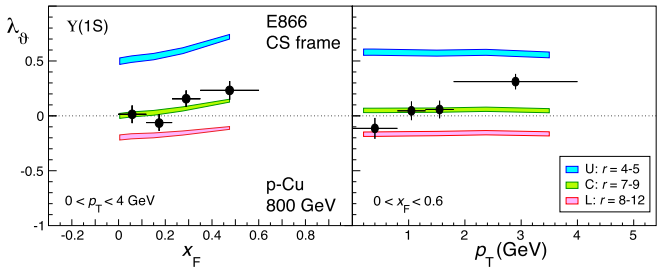

Fig. 7. Same as Fig. 6, for the $\Upsilon(1S)$ λ_ϑ parameter measured by E866 in the CS frame.

The uncertainty in the χ_c feed-down contribution has a large effect on the numerical determination of r, but almost no influence on the agreement between model and data. The interesting outcome of this comparison is that it is *possible* to describe quite accurately the J/ψ data for $x_F \lesssim 0.5$, with the only substantial hypothesis that the directly produced vector quarkonium is transversely polarized along the relative direction of the colliding q and $\overline{q}$, and longitudinally polarized along that of the colliding gluons. This conclusion is reinforced by the comparison with the $\Upsilon(1S)$ E866 measurement (λ_ϑ in the CS frame), shown in Fig. 7 for the same r values as determined using the J/ψ data. The central scenario is in very good agreement with the data. It is true that the fourth p_T point departs from the band, by around three times its uncertainty, but the significance of this difference seems to be suspiciously overestimated when we consider that the λ_ϑ value measured for p_T values only around 1 GeV lower is perfectly reproduced by the model, and that almost no physical variations should be expected within such a small p_T interval, only one tenth of the particle mass.

We remind that the χ feed-down fractions in the central scenario are fixed to the values 19% and 45%, respectively for the J/ψ and the $\Upsilon(1S)$, where the latter is only a reasonable guess, given the absence of suitable measurements. For this central scenario, the "universal" ratio between the $q\overline{q}$ and gg cross sections for quarkonium production is determined to be $r = 8 \pm 1$. The spread between the three bands (scenarios U, C, and L) is much larger in Fig. 7 than in Fig. 6 because of the very uncertain χ_b feed-down fractions.

The data-to-model comparison for the J/ψ and $\Upsilon(1S)$ mesons involves 24 data points measured as a function of x_F plus 29 points as a function of p_T. Only a couple of points have central values differing from the central-scenario curves by around two or three times their uncertainties. While it is true that not all of these measurements are statistically independent, this remains a remarkable outcome, especially given the simplicity of the model (with only one free parameter) and the diversity of measured patterns. It is fair to say, therefore, that the low-p_T J/ψ and $\Upsilon(1S)$ polarizations measured in proton-nucleus collisions can be well described by the superposition of gg fusion and $q\overline{q}$ annihilation processes, with maximally different polarizations, under a reasonable assumption for the unknown χ polarizations: all four states (χ_{c1}, χ_{c2}, χ_{b1}, and χ_{b2}) have angular momentum projections ± 1 and 0, respectively along the q–$\overline{q}$ and g–g collision directions, just as assumed for the directly produced vector mesons.

The last piece of our data-model comparison concerns the E866 measurement for the (unresolved) $\Upsilon(2S)$ and $\Upsilon(3S)$ states, shown in Fig. 8: the data are significantly above all three model scenarios. This would seem to imply that the (slightly) heavier Υ

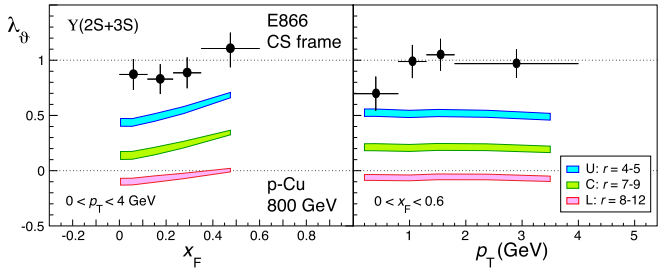

Fig. 8. Same as Fig. 7, for the Υ(2S+3S).

states evade the "universality" of the assumed physical inputs in a rather drastic way. In fact, even if we assumed that the polarizations of the $\chi_b(2P)$ and $\chi_b(3P)$ states, contributing to the production of all three $\Upsilon(nS)$ states, are extremely different from the polarizations of the $\chi_b(1P)$ states, only contributing to $\Upsilon(1S)$ production (certainly a rather unreasonable hypothesis), it would still be impossible to reproduce the data with our universal model for vector-quarkonium production; the only option would be to assume (possibly in addition) that the $q\overline{q}$ to gg cross section ratio is significantly higher for the (only slightly heavier) 2S and 3S states with respect to the 1S case, a hypothesis that would lead to a shift of all three bands towards the $\lambda_\vartheta = \pm 1$ limit.

As mentioned before, these Υ(2S+3S) measurements are clearly a notable exception in the global panorama of the existing data. Faced with this large discrepancy, we must wonder if there could be some experimental factor causing a difference between the Υ(2S+3S) measurement and the J/ψ or Υ(1S) measurements. After all, polarizations are notoriously difficult to measure and it could well be that the reported values are affected by experimental challenges. A first observation that can be made along those lines is that the J/ψ and Υ(1S) states are seen as very prominent peaks standing out of the underlying dimuon mass continuum, while the Υ(2S+3S) joint signal is not visible (as a peak) in the measured mass distribution (Fig. 1 of Ref. [43]), given the resolution and the signal-to-background ratio of the measurement. A second interesting observation is provided by the $\cos\vartheta$ distribution shown in Fig. 3-bottom of the E866 publication.[1] The curve displayed in that figure, which corresponds to the fourth p_T bin, is distinctively asymmetric, thereby not corresponding to its legend ("$1 + 0.98\cos^2\vartheta$") and, more importantly, clearly departing from the parity-conserving $1 + \lambda_\vartheta \cos^2\vartheta$ shape that must apply to the dimuons produced in decays of quakonium states. We have fitted either the negative or the positive hemispheres of the reported $\cos\vartheta$ distribution and obtained λ_ϑ values that differ from each other by more than two times the published *total* uncertainties, an indication that those uncertainties might be underestimated. Nevertheless, the large discrepancies seen in Fig. 8 between the data points and the curves representing the central scenario would not disappear even if the Υ(2S+3S) λ_ϑ uncertainties would be increased by a factor of three. It would be very valuable to redo the analysis of the E866 data, this time using the Υ(2S+3S) over Υ(1S) ratio as a function of $\cos\vartheta$, which directly provides a measurement of the *difference* between the two polarizations, with smaller systematic uncertainties thanks to the cancellation of many potential effects in the ratio [66,69]. Unfortunately, such a re-analysis is seemingly not possible [70], so that we must wait for future measurements to fully clarify this puzzle.

[1] More precisely, in the figure of the arXiv version of the paper, given that the figure in the journal publication mistakenly shows the same distribution in the Υ(1S) and Υ(2S+3S) panels.

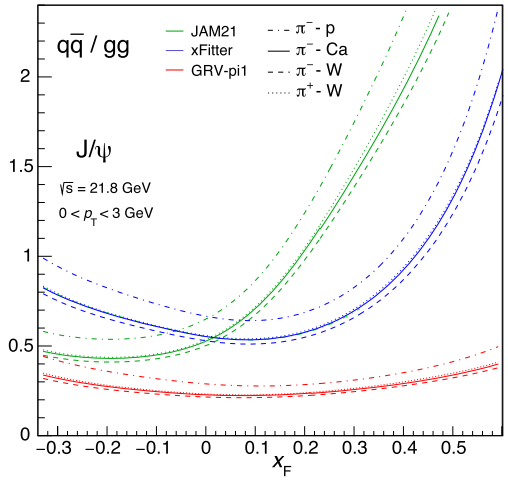

Fig. 9. The $q\overline{q}$ over gg parton luminosity ratios, vs. x_F, for J/ψ production at the collision energy of E615 [35], for the JAM21, xFitter, and GRV-pi1 pion PDF sets, and for the π^-p, π^--Ca, π^--W, and π^+-W collision systems.

6. Data vs. model for pion-nucleus collisions

Using the r values determined from the proton-nucleus data (and the same three J/ψ feed-down scenarios in which the corresponding r ranges were determined), we will now see how the model compares with the J/ψ polarization measurements performed with pion beams.

Fig. 9 shows the $q\overline{q}$ over gg parton luminosity ratios for J/ψ production, as computed using three different pion PDF sets: JAM21 [71], xFitter [72], and GRV-pi1 [73], obtained through the LHAPDF package [54]. The x_F dependence of this ratio, as well as its average value and the covered x_F range, depend quite significantly on the chosen PDF set, probably because of the poorly-known gluon density in the pion [22,23]. In comparison, the differences between positive and negative pion beams are negligible. Also the nuclear effects, computed using the EPPS16 model [55], have a minor impact, when we change the target from Ca to W, for example.

The dependence of the $q\overline{q}/gg$ ratio on the assumed PDF set directly translates into a corresponding variation in the polarization prediction, as seen in Fig. 10, where the several λ_ϑ vs. x_F and p_T bands are computed for π^--W collisions at $\sqrt{s} = 21$ GeV, using the JAM21, xFitter, and GRV-pi1 pion PDF sets. The filled bands represent the central scenario while the open ones represent the lower (solid lines) and upper (dashed lines) cases. We see that the E444 and E615 λ_ϑ measurements agree well with the model (in the $x_F \lesssim 0.5$ range) when the GRV-pi1 parton densities are used, and significantly depart from the bands representing the other two PDF sets. Incidentally, the highest x_F data points of E444 and E615 indicate a tendency towards, respectively, transverse and longitudinal polarizations (the latter having also been seen by E866 in proton-nucleus collisions). This inconsistency, independent of any model considerations, cannot be due to the different frames used in the two experiments, given that the GJ result by E615 should be intermediate between the CS and HX results of E444, reflecting the relative geometries of the three frames. Clearly, the very low J/ψ production yields close to beam rapidity must make these measurements particularly challenging. Fig. 11 completes the data to model comparison, for pion-induced collisions, by showing the corresponding results for the E537 conditions, characterized by a lower collision energy, $\sqrt{s} = 15.3$ GeV.

We clearly see that accurate polarization measurements can provide precise constraints on global fits of pion PDFs, within the context of the rather simple empirical model presented here.

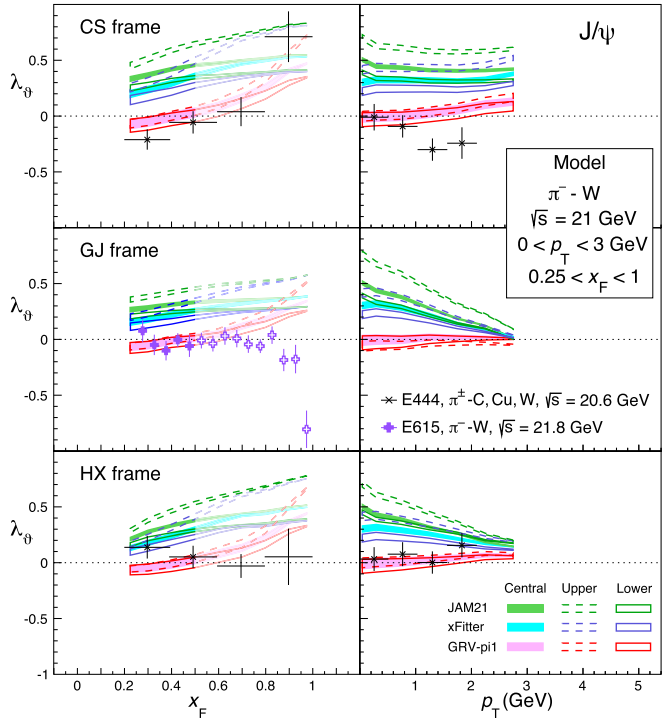

Fig. 10. The x_F and p_T dependences of the J/ψ λ_ϑ parameter, in the CS, GJ, and HX frames, as measured by E444 and E615 in π-W collisions. The bands are computed using the JAM21, xFitter, and GRV-pi1 pion PDF sets, for the three feed-down scenarios. As in Fig. 6, the data points and bands are displayed less prominently in the $x_F > 0.5$ region.

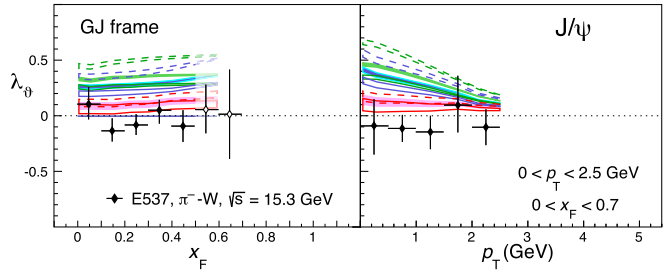

Fig. 11. Same as Fig. 10, for the E537 conditions.

7. Predictions for future measurements

New measurements in *proton*-induced collisions can validate (or falsify) the simple model we have presented in this article, where the observed polarization simply results from the interplay between $q\overline{q}$ and gg processes. After this step of model validation, also leading to a better tuning of the input parameters, improved *pion*-nucleus data should offer sensitive constraints on the pion PDFs.

The AMBER experiment at the CERN SPS accelerator, in particular, is expected to collect large samples of J/ψ events using 190 GeV proton and pion beams, with carbon and tungsten targets [24]. The top-left panel of Fig. 12 shows, for p-C collisions in the conditions of AMBER, the predicted x_F dependence of the J/ψ λ_ϑ parameter, in the CS frame, for the three feed-down scenarios considered above. We do not show the λ_φ observable because, in this frame, it is perfectly compatible with being zero and flat with p_T; correspondingly, the frame-independent parameter $\tilde{\lambda}$ [59,60] is essentially indistinguishable from λ_ϑ (and is, hence, also not shown).

The corresponding predictions for $\psi(2S)$ production are presented in the bottom-left panel. This measurement would be particularly interesting because it would test the model and constrain the pion PDFs in a cleaner and stronger way, free from the χ_c feed-down uncertainties: in this case, we simply have $\lambda_\vartheta = -1$ and $+1$ for gg fusion and $q\overline{q}$ annihilation, respectively, as for *direct* J/ψ production. The r range for $\psi(2S)$ production is assumed to be the same as for the J/ψ, indirectly depending, therefore, on the J/ψ feed-down scenario. This is why, in the figure, three sets of $\psi(2S)$ predictions are shown, despite the fact that $\psi(2S)$ production is intrinsically independent of feed-down.

The assumption that r is identical in the J/ψ and $\psi(2S)$ cases reflects the factorization hypothesis at the basis of the NRQCD and CEM approaches: possible differences between J/ψ and $\psi(2S)$ production are the result of long-distance bound-state formation effects and not of differences in the partonic cross sections.

The comparison between the J/ψ and $\psi(2S)$ predictions shows that simultaneous measurements of both polarizations in proton-nucleus collisions can be used to fix the r range *and* determine the best J/ψ feed-down scenario, at the same time.

The corresponding J/ψ and $\psi(2S)$ predictions for pion-induced collisions are shown in right panels of Fig. 12. Here, the attention should be focused on the difference between the results obtained with the three PDF sets: the spread of polarization values, on average of order $\Delta\lambda_\vartheta \simeq 0.3$, shows that the measurement should be able to significantly discriminate between existing pion PDF sets or, alternatively, provide strong constraints for future determinations of new PDF sets.

8. Summary

We have collected and reviewed the quarkonium polarization measurements reported by many fixed-target experiments, reflecting a wide variety of beams, targets, collision energies, and kinematical conditions. Given that the measurements were reported in three different polarization frames, it is not straightforward to compare them with each other, to check if they are mutually consistent and, even more importantly, to profit from the complementarity of the phase space regions that they cover to obtain more extensive and informative trends (e.g., as a function of x_F and p_T).

After a detailed look at the experimental results, seeing how they change from one polarization frame to another, and as a function of x_F, and from the J/ψ to the Υ(1S), etc., we have been able to uncover significant polarization trends, which inspired a model based on a simple hypothesis: low-p_T quarkonium production is dominated by two (2-to-1) processes, gg fusion and $q\overline{q}$ annihilation, leading, respectively, to longitudinally and transversely polarized mesons. The data-model comparisons imply accounting for the feed-down contributions from χ decays, which we have modelled with scenarios that reflect, as much as possible, the existing data (both to establish a central option and to provide a conservative uncertainty band).

Remarkably, the J/ψ and Υ(1S) data (more than 80 points measured with proton- and pion-nucleus collisions for $x_F \lesssim 0.5$) are well reproduced by this simple empirical model, with only one free parameter. On the other hand, we have been unable to reproduce, even using unreasonable variations in the feed-down contributions, the very large difference observed by E866 between the Υ(2S+3S) and Υ(1S) polarizations. Improved Υ polarization measurements would be highly desirable for a better understanding of this puzzle.

The calculations made for the comparisons with the pion-nucleus data reveal an interesting correlation between the J/ψ polarization and the assumed parton densities: the predicted polarization depends on the adopted PDF set much more than on

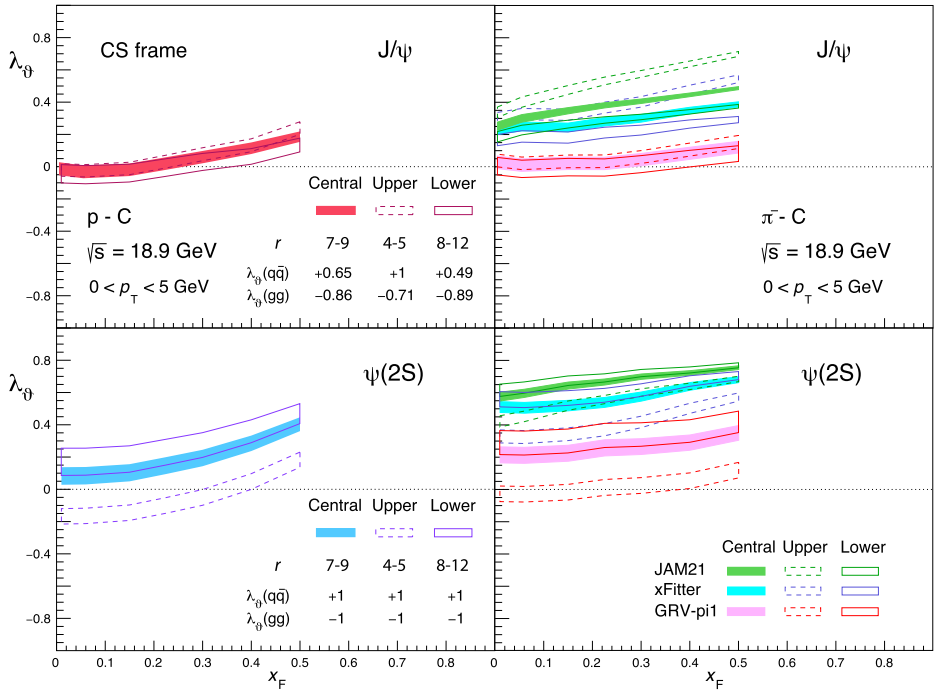

Fig. 12. The x_F dependence of the λ_ϑ parameter, in the CS frame, as predicted for J/ψ (top) and $\psi(2S)$ (bottom) production in p-C (left) and π^--C (right) collisions at $\sqrt{s} = 18.9$ GeV (corresponding to the conditions of the AMBER experiment), for the three considered J/ψ feed-down scenarios. The bands on the right panels correspond to the three pion PDF sets.

any other model input, directly reflecting the large variation of the $q\bar{q}/gg$ parton luminosity ratio, for which the three considered sets differ by a factor of 2 or more, with a strong dependence on x_F and p_T. While the GRV set reproduces reasonably well the existing data, the uncertainty represented by the differences between the three sets clearly indicates that the polarization observable has the potential to provide a strong constraint on the pion PDFs. With this motivation, we reported predictions for AMBER, an experiment that can validate (or falsify) our simple model, through improved J/ψ ("calibration") measurements in proton-nucleus collisions, and, subsequently, constrain the pion PDFs with corresponding measurements in pion-nucleus collisions. We also emphasized the important role that a measurement of the $\psi(2S)$ polarization can have, by virtue of its independence from hypotheses on the χ_c feed-down contributions, both to validate the model and to determine the pion PDFs.

We emphasise again that our study deliberately follows a data-driven approach and is exclusively focused on the polarization measurements, being fully independent of ingredients from specific theories (such as NRQCD or CEM). Our primary goal is to let the measurements indicate possible simple patterns in the polarizations of the participating processes, extracting them from the blurry global picture of the existing data. The qualitative indications we have derived in this way (e.g., quarkonia produced from $q\bar{q}$ annihilation tend to be transversely polarized while those produced from gg fusion tend to be longitudinally polarized) should encourage more sophisticated interpretations of the existing low-p_T polarization data, in the framework of present or future theory models.

Declaration of competing interest

The authors declare that they have no known competing financial interests or personal relationships that could have appeared to influence the work reported in this paper.

Data availability

No data was used for the research described in the article.

Acknowledgements

P.F. and C.L. acknowledge support from Fundação para a Ciência e a Tecnologia, Portugal, under contract CERN/FIS-PAR/0010/2019.

References

[1] N. Brambilla, et al., Heavy quarkonium: progress, puzzles, and opportunities, Eur. Phys. J. C 71 (2011) 1534, https://doi.org/10.1140/epjc/s10052-010-1534-9, arXiv:1010.5827.

[2] G. Bodwin, E. Braaten, P. Lepage, Rigorous QCD analysis of inclusive annihilation and production of heavy quarkonium, Phys. Rev. D 51 (1995) 1125, https://doi.org/10.1103/PhysRevD.51.1125, Erratum: Phys. Rev. D 55 (1997) 5853, arXiv:hep-ph/9407339.

[3] R. Baier, R. Rückl, Hadronic production of J/ψ and Υ: transverse momentum distributions, Phys. Lett. B 102 (1981) 364, https://doi.org/10.1016/0370-2693(81)90636-5.

[4] J.-P. Lansberg, On the mechanisms of heavy-quarkonium hadroproduction, Eur. Phys. J. C 61 (2009) 693, https://doi.org/10.1140/epjc/s10052-008-0826-9, arXiv:0811.4005.

[5] V.D. Barger, W.-Y. Keung, R.J.N. Phillips, On ψ and Υ production via gluons, Phys. Lett. B 91 (1980) 253, https://doi.org/10.1016/0370-2693(80)90444-X.

[6] V.D. Barger, W.-Y. Keung, R.J.N. Phillips, Hadroproduction of ψ and Υ, Z. Phys. C 6 (1980) 169, https://doi.org/10.1007/BF01588844.

[7] T. Aaltonen, et al., Measurements of angular distributions of muons from Υ meson decays in $p\bar{p}$ collisions at $\sqrt{s} = 1.96$ TeV, Phys. Rev. Lett. 108 (2012) 151802, https://doi.org/10.1103/PhysRevLett.108.151802, arXiv:1112.1591.

[8] S. Chatrchyan, et al., Measurement of the prompt J/ψ and ψ' polarizations in pp collisions at $\sqrt{s} = 7$ TeV, Phys. Lett. B 727 (2013) 381, https://doi.org/10.1016/j.physletb.2013.10.055, arXiv:1307.6070.

[9] S. Chatrchyan, et al., Measurement of the $\Upsilon(1S)$, $\Upsilon(2S)$, and $\Upsilon(3S)$ polarizations in pp collisions at $\sqrt{s} = 7$ TeV, Phys. Rev. Lett. 110 (2013) 081802, https://doi.org/10.1103/PhysRevLett.110.081802, arXiv:1209.2922.

[10] R. Aaij, et al., Measurement of J/ψ polarization in pp collisions at $\sqrt{s} = 7$ TeV, Eur. Phys. J. C 73 (2013) 2631, https://doi.org/10.1140/epjc/s10052-013-2631-3, arXiv:1307.6379.

[11] R. Aaij, et al., Measurement of $\psi(2S)$ polarisation in pp collisions at $\sqrt{s} = 7$ TeV, Eur. Phys. J. C 74 (2014) 2872, https://doi.org/10.1140/epjc/s10052-014-2872-9, arXiv:1403.1339.

[12] R. Aaij, et al., Measurement of the Υ polarizations in pp collisions at $\sqrt{s} = 7$ and 8 TeV, J. High Energy Phys. 12 (2017) 110, https://doi.org/10.1007/JHEP12(2017)110, arXiv:1709.01301.

[13] M. Butenschön, B.A. Kniehl, J/ψ polarization at Tevatron and LHC: nonrelativistic-QCD factorization at the crossroads, Phys. Rev. Lett. 108 (2012) 172002, https://doi.org/10.1103/PhysRevLett.108.172002, arXiv:1201.1872.

[14] K.-T. Chao, Y.-Q. Ma, H.-S. Shao, K. Wang, Y.-J. Zhang, J/ψ polarization at hadron colliders in nonrelativistic QCD, Phys. Rev. Lett. 108 (2012) 242004, https://doi.org/10.1103/PhysRevLett.108.242004, arXiv:1201.2675.

[15] B. Gong, L.-P. Wan, J.-X. Wang, H.-F. Zhang, Polarization for prompt J/ψ and $\psi(2S)$ production at the Tevatron and LHC, Phys. Rev. Lett. 110 (2013) 042002, https://doi.org/10.1103/PhysRevLett.110.042002, arXiv:1205.6682.

[16] M. Butenschön, B.A. Kniehl, Next-to-leading-order tests of NRQCD factorization with J/ψ yield and polarization, Mod. Phys. Lett. A 28 (2013) 1350027, https://doi.org/10.1142/S0217732313500272, arXiv:1212.2037.

[17] P. Faccioli, V. Knünz, C. Lourenço, J. Seixas, H. Wöhri, Quarkonium production in the LHC era: a polarized perspective, Phys. Lett. B 736 (2014) 98, https://doi.org/10.1016/j.physletb.2014.07.006, arXiv:1403.3970.

[18] G.T. Bodwin, K.-T. Chao, H.S. Chung, U.-R. Kim, J. Lee, Y.-Q. Ma, Fragmentation contributions to hadroproduction of prompt J/ψ, χ_{cJ}, and $\psi(2S)$ states, Phys. Rev. D 93 (2016) 034041, https://doi.org/10.1103/PhysRevD.93.034041, arXiv:1509.07904.

[19] P. Faccioli, C. Lourenço, M. Araújo, J. Seixas, I. Krätschmer, V. Knünz, From identical S- and P-wave p_T spectra to maximally distinct polarizations: probing NRQCD with χ states, Eur. Phys. J. C 78 (2018) 268, https://doi.org/10.1140/epjc/s10052-018-5755-7, arXiv:1802.01106.

[20] P. Faccioli, C. Lourenço, NRQCD colour-octet expansion vs. LHC quarkonium production: signs of a hierarchy puzzle?, Eur. Phys. J. C 79 (2019) 457, https://doi.org/10.1140/epjc/s10052-019-6968-0, arXiv:1905.09553.

[21] V. Cheung, R. Vogt, Production and polarization of direct J/ψ to $O(\alpha_s^3)$ in the improved color evaporation model in collinear factorization, Phys. Rev. D 104 (2021) 094026, https://doi.org/10.1103/PhysRevD.104.094026, arXiv:2102.09118.

[22] W.-C. Chang, J.-C. Peng, S. Platchkov, T. Sawada, Constraining gluon density of pions at large x by pion-induced J/ψ production, Phys. Rev. D 102 (2020) 054024, https://doi.org/10.1103/PhysRevD.102.054024, arXiv:2006.06947.

[23] C.-Y. Hsieh, Y.-S. Lian, W.-C. Chang, J.-C. Peng, S. Platchkov, T. Sawada, NRQCD analysis of charmonium production with pion and proton beams at fixed-target energies, Chin. J. Phys. 73 (2021) 1510, https://doi.org/10.1016/j.cjph.2021.06.001, arXiv:2103.11660.

[24] C. Quintans, The new AMBER experiment at the CERN SPS, Few-Body Syst. 63 (2022) 72, https://doi.org/10.1007/s00601-022-01769-7.

[25] S.P. Baranov, A.V. Lipatov, N.P. Zotov, Prompt charmonia production and polarization at LHC in the NRQCD with k_T-factorization. Part I: $\psi(2S)$ meson, Eur. Phys. J. C 75 (2015) 455, https://doi.org/10.1140/epjc/s10052-015-3689-x, arXiv:1508.05480.

[26] S.P. Baranov, A.V. Lipatov, N.P. Zotov, Prompt charmonia production and polarization at LHC in the NRQCD with k_T-factorization. Part II: χ_c mesons, Phys. Rev. D 93 (2016) 094012, https://doi.org/10.1103/PhysRevD.93.094012, arXiv:1510.02411.

[27] Y.-Q. Ma, R. Vogt, Quarkonium production in an improved color evaporation model, Phys. Rev. D 94 (2016) 114029, https://doi.org/10.1103/PhysRevD.94.114029, arXiv:1609.06042.

[28] V. Cheung, R. Vogt, Production and polarization of prompt J/ψ in the improved color evaporation model using the k_T-factorization approach, Phys. Rev. D 98 (2018) 114029, https://doi.org/10.1103/PhysRevD.98.114029, arXiv:1808.02909.

[29] V. Cheung, R. Vogt, Production and polarization of prompt Υ(nS) in the improved color evaporation model using the k_T-factorization approach, Phys. Rev. D 99 (2019) 034007, https://doi.org/10.1103/PhysRevD.99.034007, arXiv:1811.11570.

[30] P. Faccioli, C. Lourenço, J. Seixas, H. Wöhri, Towards the experimental clarification of quarkonium polarization, Eur. Phys. J. C 69 (2010) 657, https://doi.org/10.1140/epjc/s10052-010-1420-5, arXiv:1006.2738.

[31] S. Tzamarias, et al., ψ production in $\bar{p}N$ and $\pi^- N$ interactions at 125 GeV/c and a determination of the gluon structure functions of the $\bar{p}$ and the π^-, Phys. Rev. D 48 (1993) 5067, https://doi.org/10.1103/PhysRevD.48.5067.

[32] M.A. Abolins, et al., Production of ψ and ψ' mesons in $\pi^- N$ scattering at 150 GeV/c, Phys. Lett. B 82 (1979) 145, https://doi.org/10.1016/0370-2693(79)90446-5.

[33] R. Arnaldi, et al., J/ψ production in indium-indium collisions, Eur. Phys. J. C 43 (2005) 167, https://doi.org/10.1140/epjc/s2005-02208-y.

[34] K.J. Anderson, et al., Evidence for longitudinal photon polarization in muon pair production by pions, Phys. Rev. Lett. 43 (1979) 1219, https://doi.org/10.1103/PhysRevLett.43.1219.

[35] C. Biino, et al., J/ψ longitudinal polarization from πN interactions, Phys. Rev. Lett. 58 (1987) 2523, https://doi.org/10.1103/PhysRevLett.58.2523.

[36] J. Badier, et al., Experimental j/ψ hadronic production from 150 GeV/c to 280 GeV/c, Z. Phys. C 20 (1983) 101, https://doi.org/10.1007/BF01573213.

[37] Y.A. Alexandrov, et al., Inclusive J/ψ and ψ' production in π^--nucleus interactions at $\sqrt{s} \simeq 26$ GeV, Nucl. Phys. B 557 (1999) 3, https://doi.org/10.1016/S0550-3213(99)00412-5.

[38] A. Gribushin, et al., Production of J/ψ and $\psi(2S)$ mesons in π^--Be collisions at 515 GeV/c, Phys. Rev. D 53 (1996) 4723, https://doi.org/10.1103/PhysRevD.53.4723.

[39] A. Gribushin, et al., Production of J/ψ mesons in p-Be collisions at 530 GeV/c and 800 GeV/c, Phys. Rev. D 62 (2000) 012001, https://doi.org/10.1103/PhysRevD.62.012001, arXiv:hep-ex/9910005.

[40] T. Alexopoulos, et al., Differential cross-sections of J/ψ and $\psi(2S)$ in 800 GeV/c p-Si interactions, Phys. Rev. D 55 (1997) 3927, https://doi.org/10.1103/PhysRevD.55.3927.

[41] T.H. Chang, et al., J/ψ polarization in 800 GeV p-Cu interactions, Phys. Rev. Lett. 91 (2003) 211801, https://doi.org/10.1103/PhysRevLett.91.211801, arXiv:hep-ex/0308001.

[42] I. Abt, et al., Angular distributions of leptons from J/ψ's produced in 920 GeV fixed-target proton-nucleus collisions, Eur. Phys. J. C 60 (2009) 517, https://doi.org/10.1140/epjc/s10052-009-0957-7, arXiv:0901.1015.

[43] C.N. Brown, et al., Observation of polarization in bottomonium production at $\sqrt{s} = 38.8$ GeV, Phys. Rev. Lett. 86 (2001) 2529, https://doi.org/10.1103/PhysRevLett.86.2529, arXiv:hep-ex/0011030.

[44] J.C. Collins, D.E. Soper, Angular distribution of dileptons in high-energy hadron collisions, Phys. Rev. D 16 (1977) 2219, https://doi.org/10.1103/PhysRevD.16.2219.

[45] K. Gottfried, J.D. Jackson, On the connection between production mechanism and decay of resonances at high-energies, Nuovo Cimento 33 (1964) 309, https://doi.org/10.1007/BF02750195.

[46] P. Faccioli, Questions and prospects in quarkonium polarization measurements from proton-proton to nucleus-nucleus collisions, Mod. Phys. Lett. A 27 (2012) 1230022, https://doi.org/10.1142/S0217732312300224, arXiv:1207.2050.

[47] $\psi(2S) \to \pi^+\pi^- J/\psi$ decay distributions, Phys. Rev. D 62 (2000) 032002, https://doi.org/10.1103/PhysRevD.62.032002, arXiv:hep-ex/9909038.

[48] A high statistics study of $\Upsilon(2S) \to \pi^+\pi^-\Upsilon(1S)$, Phys. Rev. D 30 (1984) 1433, https://doi.org/10.1103/PhysRevD.30.1433.

[49] The hadronic transitions $\Upsilon(2S) \to \Upsilon(1S)$, Phys. Rev. D 58 (1998) 052004, https://doi.org/10.1103/PhysRevD.58.052004, arXiv:hep-ex/9802024.

[50] P. Faccioli, C. Lourenço, Particle Polarization in High Energy Physics: an Introduction and Case Studies on Vector Particle Production at the LHC, Lecture Notes in Physics, Springer, 2022.

[51] P. Faccioli, C. Lourenço, J. Seixas, H.K. Wöhri, Model-independent constraints on the shape parameters of dilepton angular distributions, Phys. Rev. D 83 (2011) 056008, https://doi.org/10.1103/PhysRevD.83.056008, arXiv:1102.3946.

[52] P. Faccioli, C. Lourenço, J. Seixas, H.K. Wöhri, Determination of χ_c and χ_b polarizations from dilepton angular distributions in radiative decays, Phys. Rev. D 83 (2011) 096001, https://doi.org/10.1103/PhysRevD.83.096001, arXiv:1103.4882.

[53] S. Dulat, T.-J. Hou, J. Gao, M. Guzzi, J. Huston, P. Nadolsky, J. Pumplin, C. Schmidt, D. Stump, C.P. Yuan, New parton distribution functions from a global analysis of quantum chromodynamics, Phys. Rev. D 93 (2016) 033006, https://doi.org/10.1103/PhysRevD.93.033006, arXiv:1506.07443.

[54] A. Buckley, J. Ferrando, S. Lloyd, K. Nordström, B. Page, M. Rüfenacht, M. Schönherr, G. Watt, LHAPDF6: parton density access in the LHC precision era, Eur. Phys. J. C 75 (2015) 132, https://doi.org/10.1140/epjc/s10052-015-3318-8, arXiv:1412.7420.

[55] K.J. Eskola, P. Paakkinen, H. Paukkunen, C.A. Salgado, EPPS16: nuclear parton distributions with LHC data, Eur. Phys. J. C 77 (2017) 163, https://doi.org/10.1140/epjc/s10052-017-4725-9, arXiv:1612.05741.

[56] E.L. Berger, S.J. Brodsky, Quark structure functions of mesons and the Drell–Yan process, Phys. Rev. Lett. 42 (1979) 940, https://doi.org/10.1103/PhysRevLett.42.940.

[57] E.L. Berger, Quark structure functions of mesons, fragmentation functions, higher twist effects in QCD, deep inelastic scattering, and the Drell–Yan process, Z. Phys. C 4 (1980) 289, https://doi.org/10.1007/BF01421570.

[58] Kinematic distributions and nuclear effects of J/ψ production in 920 GeV fixed-target proton-nucleus collisions, Eur. Phys. J. C 60 (2009) 525, https://doi.org/10.1140/epjc/s10052-009-0965-7, arXiv:0812.0734.

[59] P. Faccioli, C. Lourenço, J. Seixas, Rotation-invariant relations in vector meson decays into fermion pairs, Phys. Rev. Lett. 105 (2010) 061601, https://doi.org/10.1103/PhysRevLett.105.061601, arXiv:1005.2601.

[60] P. Faccioli, C. Lourenço, J. Seixas, New approach to quarkonium polarization studies, Phys. Rev. D 81 (2010) 111502(R), https://doi.org/10.1103/PhysRevD.81.111502, arXiv:1005.2855.

[61] Production of the charmonium states χ_{c1} and χ_{c2} in proton nucleus interactions at $\sqrt{s}$ = 41.6 GeV, Phys. Rev. D 79 (2009) 012001, https://doi.org/10.1103/PhysRevD.79.012001, arXiv:0807.2167.

[62] A. Abulencia, et al., Measurement of $\sigma_{\chi_{c2}} \mathcal{B}(\chi_{c2} \to J/\psi\gamma)/\sigma_{\chi_{c1}} \mathcal{B}(\chi_{c1} \to J/\psi\gamma)$ in $p\bar{p}$ collisions at $\sqrt{s} = 1.96$ TeV, Phys. Rev. Lett. 98 (2007) 232001, https://doi.org/10.1103/PhysRevLett.98.232001, arXiv:hep-ex/0703028.

[63] Measurement of the ratio of prompt χ_c to J/ψ production in pp collisions at $\sqrt{s} = 7$ TeV, Phys. Lett. B 718 (2012) 431, https://doi.org/10.1016/j.physletb.2012.10.068, arXiv:1204.1462.

[64] Study of χ_b meson production in pp collisions at $\sqrt{s} = 7$ and 8 TeV and observation of the decay $\chi_b(3P) \to \Upsilon(3S)\gamma$, Eur. Phys. J. C 74 (2014) 3092, https://doi.org/10.1140/epjc/s10052-014-3092-z, arXiv:1407.7734.
[65] P. Faccioli, C. Lourenço, M. Araújo, J. Seixas, Universal kinematic scaling as a probe of factorized long-distance effects in high-energy quarkonium production, Eur. Phys. J. C 78 (2018) 118, https://doi.org/10.1140/epjc/s10052-018-5610-x, arXiv:1802.01102.
[66] A.M. Sirunyan, et al., Constraints on the χ_{c1} versus χ_{c2} polarizations in proton-proton collisions at $\sqrt{s} = 8$ TeV, Phys. Rev. Lett. 124 (2020) 162002, https://doi.org/10.1103/PhysRevLett.124.162002, arXiv:1912.07706.
[67] P.L. Cho, A.K. Leibovich, Color octet quarkonia production, Phys. Rev. D 53 (1996) 150, https://doi.org/10.1103/PhysRevD.53.150, arXiv:hep-ph/9505329.
[68] P.L. Cho, A.K. Leibovich, Color octet quarkonia production. II, Phys. Rev. D 53 (1996) 6203, https://doi.org/10.1103/PhysRevD.53.6203, arXiv:hep-ph/9511315.
[69] P. Faccioli, C. Lourenço, T. Madlener, From prompt to direct J/ψ production: new insights on the χ_{c1} and χ_{c2} polarizations and feed-down contributions from a global-fit analysis of mid-rapidity LHC data, Eur. Phys. J. C 80 (2020) 623, https://doi.org/10.1140/epjc/s10052-020-8201-6, arXiv:2006.15446.
[70] M. Leitch (spokesperson of the E866 Collaboration), private communication.
[71] P.C. Barry, N. Sato, W. Melnitchouk, C.-R. Ji, First Monte Carlo global QCD analysis of pion parton distributions, Phys. Rev. Lett. 121 (2018) 152001, https://doi.org/10.1103/PhysRevLett.121.152001, arXiv:1804.01965.
[72] I. Novikov, et al., Parton distribution functions of the charged pion within the xFitter framework, Phys. Rev. D 102 (2020) 014040, https://doi.org/10.1103/PhysRevD.102.014040, arXiv:2002.02902.
[73] M. Gluck, E. Reya, A. Vogt, Pionic parton distributions, Z. Phys. C 53 (1992) 651, https://doi.org/10.1007/BF01559743.